Development 138, 767-776 (2011) doi:10.1242/dev.057588

Disruption of reelin signaling alters mammary gland morphogenesis

Elvira Khialeeva[1], Timothy F. Lane[2] and Ellen M. Carpenter[1,*]

SUMMARY

Reelin signaling is required for appropriate cell migration and ductal patterning during mammary gland morphogenesis. Dab1, an intracellular adaptor protein activated in response to reelin signaling, is expressed in the developing mammary bud and in luminal epithelial cells in the adult gland. Reelin protein is expressed in a complementary pattern, first in the epithelium overlying the mammary bud during embryogenesis and then in the myoepithelium and periductal stroma in the adult. Deletion in mouse of either *reelin* or *Dab1* induced alterations in the development of the ductal network, including significant retardation in ductal elongation, decreased terminal branching, and thickening and disorganization of the luminal wall. At later stages, some mutant glands overcame these early delays, but went on to exhibit enlarged and chaotic ductal morphologies and decreased terminal branching: these phenotypes are suggestive of a role for reelin in spatial patterning or structural organization of the mammary epithelium. Isolated mammary epithelial cells exhibited decreased migration in response to exogenous reelin in vitro, a response that required *Dab1*. These observations highlight a role for reelin signaling in the directed migration of mammary epithelial cells driving ductal elongation into the mammary fat pad and provide the first evidence that reelin signaling may be crucial for regulating the migration and organization of non-neural tissues.

KEY WORDS: Reeler, Dab1, Mammary epithelial cell, Ductal branching, Ductal elongation, Extracellular matrix, Mouse

INTRODUCTION

Reelin signaling has been identified as a key factor in regulating cell migration and positioning throughout the central nervous system (Caviness and Sidman, 1973; Caviness, 1976; Goffinet, 1984; Yip et al., 2000; Phelps et al., 2002). Anatomical examination of the brain and spinal cord in *reeler* mice, which carry a naturally occurring deletion mutation in the *reelin* gene (D'Arcangelo et al., 1995), has revealed defects including a lack of foliation and reduction in the size of the cerebellum, disrupted lamination in the hippocampus, inverted cortical lamination and abnormal positioning of nuclei in the brain and spinal cord (reviewed by D'Arcangelo and Curran, 1998; Rice and Curran, 2001). Observations on cellular activities governed by reelin signaling have been largely restricted to the nervous system, but recent studies have suggested a number of non-neuronal activities for reelin signaling. The *reelin* gene is expressed in odontoblasts, where it may mediate terminal innervation of tooth pulp (Maurin et al., 2004). Reelin is also frequently silenced in pancreatic cancer, and knockdown of multiple components of the reelin signaling pathway leads to increased cell motility and invasiveness in pancreatic cancer cells (Sato et al., 2006). Several isoforms of Dab1 are expressed in non-neural tissues such as kidney, liver and limbs in mice and zebrafish (Costagli et al., 2006; Howell et al., 1997a) suggesting possible additional roles for reelin signaling in the development of these structures.

We have explored a role for reelin signaling in the development and morphogenesis of the mammary gland. Mammary glands are skin appendages that develop via extensive epithelial-mesenchymal interactions (reviewed by Mikkola and Millar, 2006; Robinson, 2007). During embryogenesis, epithelially derived mammary placodes invaginate into the underlying mesenchyme to produce mammary buds. These buds then proliferate and extend into the mesenchyme to produce the mammary sprout. Once the sprout reaches the underlying stromal fat pad, it begins to branch and a lumen forms within the epithelium to generate a primary ductal tree. The ductal tree is quiescent until the onset of puberty, at which time the gland enters a period of extensive growth and branching to form a mature ductal network that completely fills the fat pad. During the process of ductal elongation and branching, the ducts are tipped with terminal end buds, club-shaped bilayered epithelial structures that are the site of rapid cell proliferation (Ball, 1998). Retraction of these buds occurs once ductal growth is complete and the mature branching pattern has been established.

Growth and extension of mammary ducts requires extensive communication between epithelial and mesenchymal components of the gland. Mammary mesenchyme induces the overlying epithelium to form the mammary buds, probably by inducing epithelial cell migration and changes in epithelial cell shape (reviewed by Cunha, 1994). Interactions between the epithelium and the stroma then dictate the terminal branching pattern of the ducts (Naylor and Ormandy, 2002). Cavitation of the ducts also involves epithelial-mesenchymal interactions, as epithelial cells in contact with the surrounding basal lamina become organized into the luminal epithelium, whereas those that lose contact undergo apoptosis to clear the center of the lumen (reviewed by Gjorevski and Nelson, 2009). Cell-matrix interactions are mediated by a variety of cell adhesion molecules and these interactions are crucial in establishing the specific expression of milk protein genes in the mammary gland (Streuli

[1]Department of Psychiatry and Biobehavioral Science and [2]Departments of Biological Chemistry and Obstetrics and Gynecology, UCLA School of Medicine, Los Angeles, CA 90095, USA.

*Author for correspondence (ecarpenter@mednet.ucla.edu)

Accepted 3 December 2010

et al., 1995). Thus, epithelial-mesenchymal interactions are required for the development, shaping and maturation of the mammary gland.

In this study, we have identified a role for reelin, a large extracellular matrix glycoprotein, and the reelin signaling pathway in the morphogenesis of the mammary gland. In the nervous system, reelin signaling is initiated by the deposition of reelin into the extracellular matrix. Reelin then binds to multimeric complexes of two low-density lipoprotein receptors, ApoER2 and VLDLR (reviewed by Herz and Chen, 2006). Signal transduction is mediated through the Dab1 intracellular adaptor protein, which is phosphorylated in response to reelin signaling primarily by Src family kinases (Howell et al., 1999; Kuo et al., 2005). Phosphorylated Dab1 activates a cascade of events that ultimately inhibits tau phosphorylation and promotes microtubule stabilization in the cytoskeleton, thus triggering the cessation of migration. In the absence of reelin signaling, neurons mis-migrate, producing numerous errors in cell positioning and cell layering (e.g. Caviness and Sidman, 1973; Caviness, 1976; Goffinet et al., 1984; Yip et al., 2000; Phelps et al., 2002; Förster et al., 2006). In our current study, we have demonstrated that reelin signaling pathway components are expressed in and around the mammary bud, with Dab1 expressed in invaginating placodal cells and reelin expressed in the overlying epithelium. Expression continues postnatally, with reelin in the mesenchymally derived periductal stroma and myoepithelial cells, and Dab1 in the luminal mammary epithelial cells lining the developing ducts. *Reelin* and *Dab1* genes are both required for normal mammary gland morphogenesis, as disruptions in either of these genes produces delays in ductal extension and chaotic ductal morphology. We have also shown that migration of isolated mammary epithelial cells is inhibited by exogenous reelin. These studies demonstrate an important role for reelin signaling in mammary gland morphogenesis and provide the first evidence that reelin signaling has the capacity to regulate the migration and organization of non-neural tissue.

MATERIALS AND METHODS

Mouse lines

Reeler mice (B6C3Fe-*a*/*a*-*Reln*^{rl}/J) were obtained from the Jackson Laboratory (Bar Harbor, ME, USA). Two types of *Dab1* mice were used. CBy.12954-*Dab1*^{tm1Cpr}/J mice, which carry a disruption of the protein interaction/protein binding domain of *Dab1* (Howell et al., 1997a; Howell et al., 1997b) were obtained from the Jackson Laboratory. *Dab1*^{exKIneo} mice, in which a *lacZ* reporter gene replaces exon 1 of *Dab1*, were kindly provided by Dr Brian Howell (Pramatarova et al., 2008). *Dab1* mutant mice were used interchangeably for anatomical analysis, as the mutant phenotypes are indistinguishable in the two lines. *lacZ* gene expression was analyzed exclusively in *Dab1*^{exKIneo} mice. *Reeler* and *Dab1*^{exKIneo} mice are maintained on a C57Bl/6 background, whereas *Dab1*^{tm1Cpr}/J mice are maintained on a Balb/C background. Homozygous mutant mice and wild-type controls were obtained by intercrossing heterozygous parents. Offspring from *reeler* and CBy.12954-*Dab1*^{tm1Cpr}/J intercrosses were genotyped by PCR as described (D'Arcangelo et al., 1995; Howell et al., 1997a). *Dab1*^{exKIneo} intercross offspring were genotyped using the following primers: Ngen04, 5′-TGATGCTATCCCTAGCAAGAC-3′; Exon3 Rev, 5′-GTGGCTTCGCTGCGATCCTGAC-3′; CKO R3, 5′-CTTGAAGACGAAAGGGCCT-3′.

X-Gal staining, immunohistochemistry and histology

lacZ gene expression was visualized in formalin-fixed whole embryos, and 20-40 μm tissue sections, following overnight incubation in a bromo-chloro-indolyl-galactopyranoside (X-Gal) reaction buffer composed of 1 mg/ml X-Gal in 5 mM $K_3Fe(CN)_6$, 5 mM $K_4Fe(CN)_6$-$3H_2O$, 1 mM $MgCl_2$, 0.01% deoxycholic acid (DOC) and 0.02% Igepal (Sigma, USA). For immunohistochemistry, tissue sections were reacted to reveal X-Gal as above, post-fixed briefly with 4% paraformaldehyde, then incubated overnight with primary antibodies diluted in 1× PBS + 10% dry milk powder. Horseradish peroxidase (HRP)-conjugated secondary antibodies (Jackson ImmunoResearch, West Grove, PA, USA) were diluted 1:250 in PBS+10% dry milk powder and incubated for 2-4 hours at room temperature. HRP was visualized using diaminobenzidine. Paraffin sections were dewaxed and rehydrated through graded ethanols. Antigen retrieval was performed by boiling for 10 minutes in Tris-HCl buffer, then sections were incubated for 60 minutes with primary antibodies diluted in 1% bovine serum albumin in Tris-buffered saline. Streptavidin-conjugated secondary antibody incubation and HRP visualization were performed following the manufacturer's instructions (Dako NA, Carpinteria, CA, USA). Primary antibody dilutions were as follows: anti-reelin (Millipore, Billerica, MA USA) 1:500; anti-Dab1 (Millipore) 1:500, anti-K14 (Covance, Princeton, NJ, USA) 1:1000; anti-K8/18 (ProGen, Germany) 1:300; anti-NKCC1 (gift of Dr Jim Turner, National Institute of Craniofacial and Dental Research, NIH, Bethesda, MD, USA) 1:1000; anti-Ki67 (Vector Laboratories, Burlingame, CA, USA), 1:1000. For histology, 7 μm paraffin sections were stained using hematoxylin and eosin.

RT-PCR

Mammary buds were dissected from abdominal walls of embryonic day 13.5 (E13.5) embryos and were flash-frozen. Buds collected from three embryos of the same genotype were pooled and total RNA was extracted using RNA Wiz as described (Anderson et al., 2002), reverse transcribed using Superscript II (Invitrogen, Carlsbad, CA, USA), then amplified using the following primers: ApoER2 forward, 5′-AGCGTTTGTACTGGGTG-GAC-3′; ApoER2 reverse, 5′-GCTGGAGATTTGAGGAGCAG-3′; VLDLR forward, 5′-ACGGCCAGTGTGTTCCTAAC-3′; VLDLR reverse, 5′-CCATCGTCACAGTCATCCTG-3′.

Carmine Red staining and branch analysis

Whole mammary glands were collected and stained as previously described (Li et al., 2002). The extent of fat pad colonization was determined by measuring the length and width of the stromal fat pad, and the length and width of the ductal tree at its widest extent. Areas for both fat pad and ductal tree were calculated and the ratio of ductal tree:fat pad was determined. Terminal end buds and terminal branches were counted from photomicrographs of the entire gland.

Mammary gland transplantation

Mammary glands from six 3-week-old Balb/C host females were cleared of endogenous epithelium as described (DeOme et al., 1959). Donor mammary glands were collected from adult wild-type and *Dab1*^{tm1Cpr}/J mutants and dissected into small fragments. Wild-type and *Dab1*^{tm1Cpr}/J mutant mammary fragments were transplanted into the cleared fat pads, with each host mouse receiving a wild-type transplant and a contralateral *Dab1*^{tm1Cpr}/J mutant transplant. After 6 weeks, host mammary glands were removed and processed for whole-mount Carmine Red staining as described above.

MEC isolation and culture

Primary mammary epithelial cells (MECs) were isolated from freshly dissected mammary glands obtained from females at 13 days of gestation. Minced tissues were incubated in a digestion buffer containing collagenase and hyaluronidase for 6 hours, then digested with Dispase, filtered through 100 μm mesh tissue strainers and grown in MEC media as described (Hu et al., 2005). To ensure that isolated cells were primarily MECs, primary cultures were initially plated for 1 hour to allow fibroblasts to adhere to the culture flask. Suspended MECs were then transferred to a fresh flask and allowed to adhere. After 4 days in primary culture, MECs were serum-starved for 24 hours, then 10^5 MECs were plated into the top well of a transwell chamber. For live-cell assays, the bottom chamber contained live cells, either reelin-secreting pCrl cells (D'Arcangelo et al., 1999) (kindly provided by Dr Tom Curran, University of Pennsylvania, Philadelphia, PA, USA) or control mock-transfected 293T cells. For conditioned media cultures, media was collected from pCrl or 293T cells after 3 days of culture.

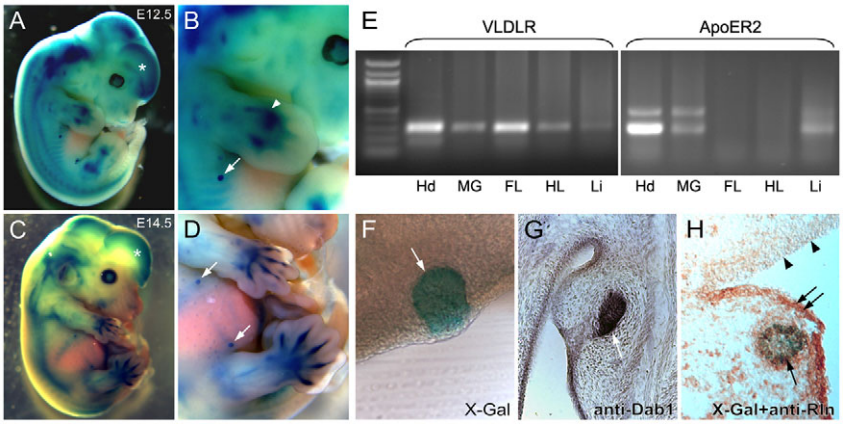

Fig. 1. Expression of reelin signaling pathway components in the embryonic mammary gland. (**A-D**) *Dab1* reporter gene expression in whole embryos at E12.5 (A,B) and E14.5 (C,D). Reporter gene expression is evident in the forebrain (A,C, asterisks), in the developing limb (B, arrowhead) and in the mammary placodes (B,D, arrows). B and D are higher magnification lateral views of the embryos in A and C, respectively. (**E**) RT-PCR detection of VLDLR and ApoER2 in wild-type E13.5 embryonic tissues. (**F**,**G**) Mammary buds at E14.5 visualized for *lacZ* reporter gene expression (F, arrow) and anti-Dab1 immunohistochemistry (G, arrow). (**H**) Double labeling for the *Dab1*^{lacZ} reporter gene (blue, arrow) and anti-reelin (brown, double arrows). Reelin is expressed in the abdominal epithelium but is excluded from the adjacent limb epithelium (arrowheads). FL, forelimb; Hd, head; HL, hindlimb; Li, liver; MG, mammary gland.

RESULTS

Reelin signaling pathway components are expressed in the mammary gland

To determine if reelin signaling might be involved in mammary gland development, we first examined the expression of reelin signaling pathway components in the embryonic mammary gland. Using a *Dab1*^{lacZ} reporter mouse [*Dab1*^{exKIneo} (Pramatarova et al., 2008)], we found that Dab1 was expressed in mammary buds in mouse embryos (Fig. 1A-D), with expression evident as early as E12.5. Reporter gene expression was limited to the mammary bud itself, with no expression in the surrounding epithelial or mesodermal tissues (Fig. 1F). Immunohistochemical labeling with anti-Dab1 antibodies also labeled the mammary buds (Fig. 1G), confirming the fidelity of reporter gene expression. Reelin expression appeared at low levels in the condensing mesenchyme surrounding the mammary bud, as well as at higher levels in the overlying epithelium. Reelin expression was specific to the epithelium of the abdominal wall, and was excluded from adjacent limb bud epithelium (Fig. 1H). ApoER2 and VLDLR were also expressed in the developing mammary bud (Fig. 1E). These observations suggest that many key elements of the reelin signaling pathway, including reelin itself, Dab1, ApoER2 and VLDLR are expressed during embryonic mammary gland development.

Next, we investigated whether reelin signaling might be active during postnatal mammary gland morphogenesis. We found that in adults, Dab1 was expressed in the adult luminal epithelium (Fig. 2A,G), where it colocalized with K8/18, a luminal cell marker (Fig. 2E). Reelin was expressed in the periductal stroma (Fig. 2B,H), complementary to where Dab1 was expressed and overlapping the expression of K14, a basal cell marker (Fig. 2F). The *lacZ* reporter gene was also expressed in adult tissue sections, and double labeling for β-galactosidase and anti-reelin expression illustrated the complementary expression patterns (Fig. 2C,D). This localization suggests a continued role for reelin signaling during postnatal mammary gland morphogenesis.

Loss of reelin signaling disrupts ductal tree formation

To determine if loss of reelin signaling affects mammary gland development, we examined *reeler* mutant mice and *Dab1* knockout mice for possible effects on mammary gland morphogenesis.

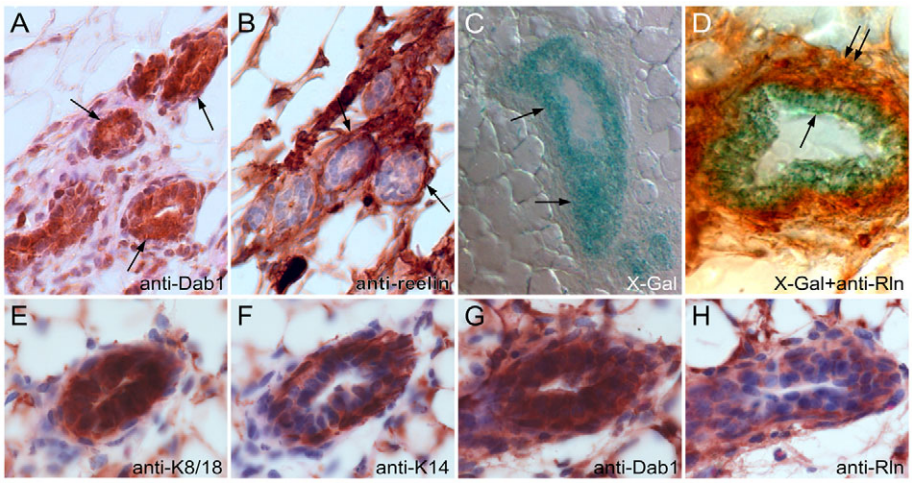

Fig. 2. *reelin* and *Dab1* expression in the adult mammary gland. (**A-D**) Dab1 is expressed in the luminal epithelium of adult females (A,C,D arrows). Reelin (B,D) is expressed in a complementary pattern in the periductal stroma (B, arrow; D, double arrow). (**E-H**) Serial sections through the same duct labeled for K8/18 (E), K14 (F), Dab1 (G) and reelin (H) confirm that Dab1 is expressed in the luminal cells and reelin is expressed in the periductal stroma.

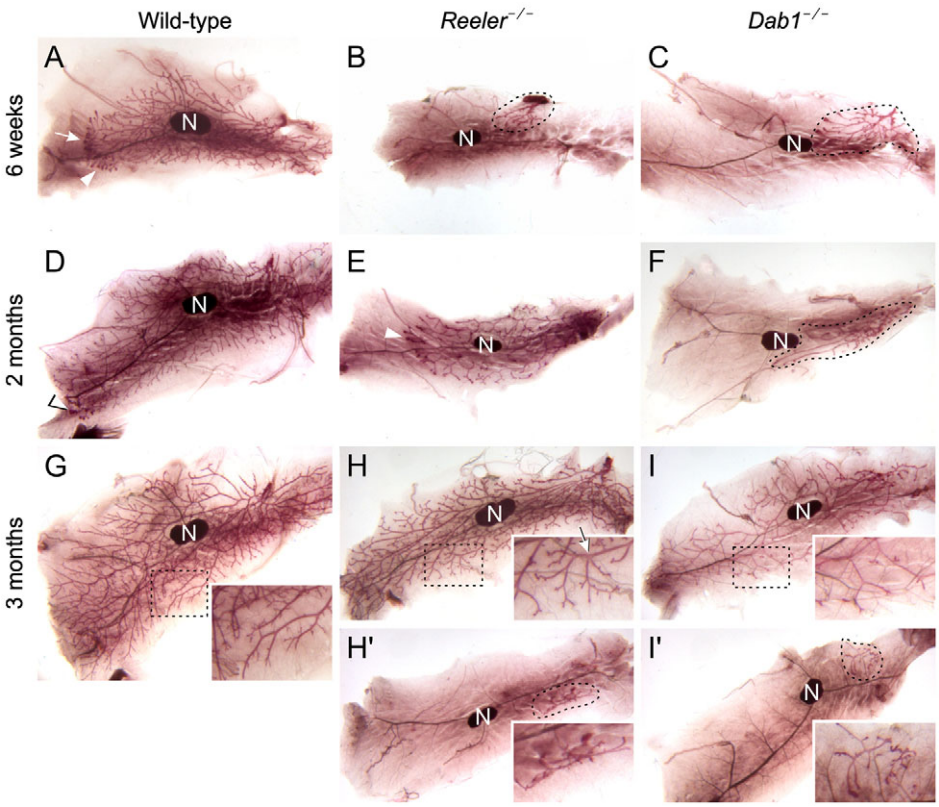

Fig. 3. Loss of *reelin* and *Dab1* expression delays and disrupts ductal tree formation. (**A**) Wild-type mammary gland with immature ductal arborization. Arrowheads indicate TEBs. (**B**,**C**) *Reeler* and *Dab1* mutant mammary glands with rudimentary ductal arborization. Mammary ducts are indicated with the dotted outlines. (**D**) Wild-type mammary gland with mature arborization. The arrowhead indicates a distal TEB. (**E**) *Reeler* mutant mammary gland with immature arborization. The arrowhead indicates a TEB. (**F**) *Dab1* mutant mammary gland with rudimentary ductal arborization. Mammary ducts are indicated by the dotted outline. (**G**) Wild-type mammary gland with mature arborization. The inset shows higher magnification of the terminal branches in the outlined area. (**H**,**H′**) *Reeler* mutant mammary glands with mature (H) and rudimentary (H′) ductal arborization. Insets show terminal branching (H) or the complete ductal network (H′). An abnormal branch point is indicated by the arrow in the H inset. (**I**,**I′**) *Dab1* mutant mammary glands with mature (I) and rudimentary (I′) arborization. Insets show terminal branching (I) or the complete ductal network (I′). All panels show the #4 inguinal mammary gland, oriented with the nipple to the right. N, inguinal lymph node.

Sections taken through *reeler* and *Dab1* embryos suggested that the initial stages of mammary gland development, i.e. mammary bud formation and invagination, were normal (data not shown); therefore we focused on postnatal mammary glands. At 6 weeks of age, wild-type glands contained an extensive ductal network, extending from the nipple well past the inguinal lymph node into the distal fat pad (Fig. 3A). Many distal branches were tipped with terminal end buds (TEBs), suggesting that active ductal growth was in progress. By contrast, both *reeler* and *Dab1* mutant glands had very small ductal trees that rarely extended even as far as the lymph node (Fig. 3B,C). TEBs were observed at the ends of some branches (Fig. 3C), but branches without TEBs were also observed. By 2 months of age, wild-type glands were fully colonized, with profusely branched ducts extending to the distal end of the fat pad, and most TEBs had regressed, indicating that ductal branching and extension was nearly complete (Fig. 3D). By comparison, at the same age, many mutant glands had small, underdeveloped ductal trees (Fig. 3E,F). As seen at 6 weeks, some distal branches were tipped with TEBs, but others were not. At 3 months of age, wild-type gland ductal branching patterns were not qualitatively different from those seen at 2 months of age (Fig. 3G). However, no TEBs were observed in wild-type glands at this age, indicating that the glands are fully mature. Mutant animals at 3 months of age showed a variety of phenotypes. Some mutant glands had fat pads that were fully colonized by a ductal network (Fig. 3H,I), whereas others had only rudimentary ductal trees (Fig. 3H′,I′). However, even in mutants with fully colonized ducts, the distal branching patterns were qualitatively different from those seen in wild-type mice. These differences were not due to differences in estrous cycle phase. Ductal arborization appeared to be less extensive than that in wild-type glands, distal branches appeared sparser (insets, Fig. 3H,I) and occasionally there were multiple branches extending from the same location (Fig. 3H, inset). TEBs were usually not present in mutant animals at this age. These observations suggest that initial ductal extension is delayed in all mutant animals. In some cases, the early delays were apparently overcome and the animals were able to develop more extensive ductal trees, whereas in others, rudimentary ductal trees were retained well into adulthood. The absence of TEBs in mutants at later ages suggests that despite the apparent failure in ductal extension, the glands have reached maturity.

To quantify the differences in ductal development, we first determined whether mammary glands had rudimentary ducts, immature ducts, or mature ductal trees. Rudimentary ducts had few branches, and no ductal extension past the level of the lymph node (e.g. Fig. 3H′,I′), immature ducts showed sparse branching patterns and occasional TEBs (e.g. Fig. 3E), whereas mature ductal trees had profuse branches and no evidence of TEBs (e.g. Fig. 3G). At 6 weeks of age, about 65% of control wild-type glands had immature ductal patterns, whereas the remainder exhibited mature ductal trees (Fig. 4A). By contrast, rudimentary ducts were seen in almost all *reeler* and *Dab1* mutants. At 2 and 3 months of age, all of the control glands had mature ductal trees, whereas a substantial fraction of mutant animals exhibited either rudimentary or immature ductal trees (Fig. 4A). Even at 3 months of age, rudimentary and immature ductal trees were still observed in mutant animals.

Second, we quantified the area of the fat pad occupied by the ductal network. At 6 weeks of age, mammary ducts filled an average of 76% of the wild-type fat pad, whereas *reeler* and *Dab1* mutant mammary fat pads were on average 12.94 and 9.83% colonized, respectively (Fig. 4B). By 2 months of age, wild-type glands were fully colonized with ducts. Although some mutant glands were also fully colonized, five of seven *reeler* mutant glands were only partially colonized, with the extent of colonization ranging from 21.23 to 87.92%, and two of five *Dab1* mutant glands

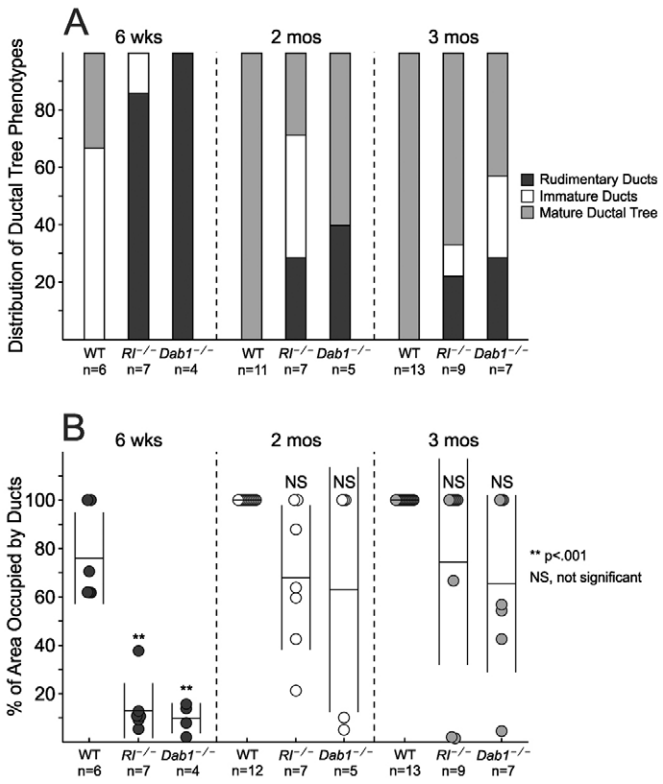

Fig. 4. Mutant animals have rudimentary or immature ducts and show decreased fat pad colonization. (**A**) Distribution of rudimentary, immature and mature ductal branching phenotypes in wild-type, *reeler* (*Rl*$^{-/-}$) and *Dab1*$^{-/-}$ mice at 6 weeks, 2 months and 3 months of age. (**B**) Quantification of the fat pad area occupied by ductal branches in wild-type, *Rl*$^{-/-}$, and *Dab1*$^{-/-}$ mammary glands at 6 weeks, 2 months and 3 months of age. Horizontal bars across each group of points designate the average area occupied, with the standard deviation indicated by vertical bars flanking each group of points. Significance was determined using *t* test comparisons between wild-type and mutant groups assuming unequal variance. WT, wild type.

were minimally colonized, with colonization ranging from 5.00 to 10.04%. At three months of age, a number of mutant glands continued to show only partial ductal colonization (three of nine reeler glands, 1.53–66.67% of area colonized; four of seven *Dab1* mutant glands, 4.49–56.73% of area colonized), whereas all wild-type glands were fully colonized. These observations suggest that persistent changes in mammary gland colonization occur in the absence of reelin signaling.

Loss of reelin signaling disrupts gland maturation and ductal branching

During mammary gland morphogenesis, ductal growth is heralded by the formation of TEBs, enlarged bilaminar structures at the distal tips of growing ducts (Ball, 1998). TEBs are present during active ductal growth and are resorbed once the ducts have completed their growth (Sternlicht et al., 2006). At 6 weeks of age, five of seven wild-type glands had visible TEBs (Fig. 5A). The remaining two glands were those glands that were 100% colonized by ducts, and had no visible TEBs. We interpret this to mean that ductal development in these glands was complete and that the TEBs had been resorbed. At the same age, all mutant glands examined had visible TEBs. Comparison of the number of TEBs in each type of gland showed that mutants had significantly fewer TEBs than wild-type animals (Fig. 5A). At 2 months of age, only three of 12 wild-type glands had TEBs, with an average of 6.7 TEBs per animal. In comparison, six of seven reeler mutant glands and two of four *Dab1* mutant glands had visible TEBs (Fig. 3E), with an average of 5.9 TEBs per gland. TEBs were also examined in histological sections to determine if there were alterations in morphology in mutant animals. At two months of age, both *reeler*$^{-/-}$ and *Dab1*$^{-/-}$ gland had terminal end buds resembling those seen in 6-week-old wild-type animals (Fig. 5C-E). TEBs were tipped with a thin cap cell layer, which transitioned to a thicker myoepithelial layer at the collar of the TEB. The TEB distribution suggests two possibilities: either that at 2 months of age, both wild-type and mutant ductal tree development is nearly complete, with only a few residual TEBs remaining; or that, because mutant glands have fewer terminal branches (see below), active growth is continuing, albeit with fewer ducts being extended. The normal TEB morphology seen in mutant glands supports the latter possibility. By 3 months of age, TEBs were not seen in *reeler* mutant glands, whereas four of eight *Dab1* mutant glands still had discernible TEBs, with an average of 8.3 TEBs per gland. This observation suggests that ductal growth may be complete in *reeler* mutants at this age, whereas development continues in *Dab1* mutants.

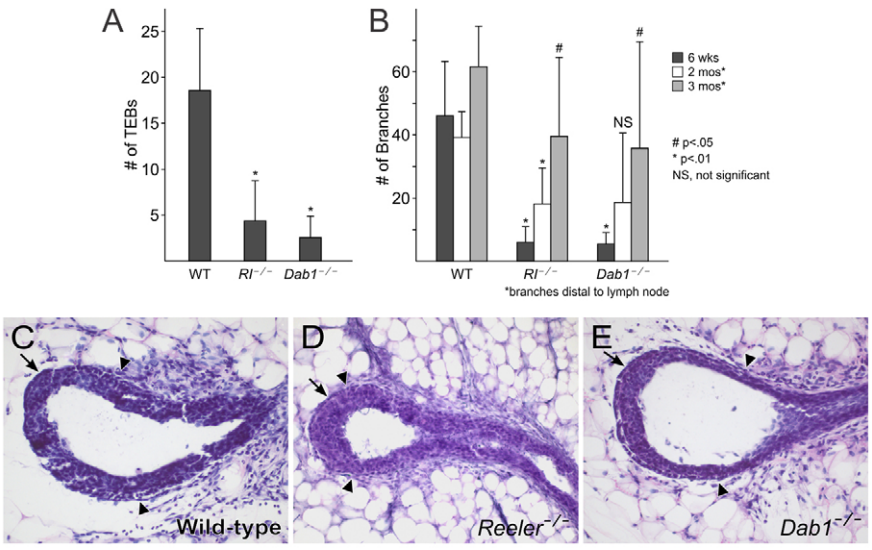

Fig. 5. TEB distribution and morphology. (**A**,**B**) TEBs were counted in 6-week-old mammary glands (A), whereas terminal branches were counted at 6 weeks, 2 months and 3 months of age (B). For 2- and 3-month-old glands, only those terminal branches extending past the level of the inguinal lymph node were counted. WT: *n*=7 (6 weeks), *n*=12 (2 months), *n*=7 (3 months); *Rl*$^{-/-}$: *n*=7 (6 weeks), *n*=7 (2 months), *n*=8 (3 months); *Dab1*$^{-/-}$ *n*=5 (6 weeks), *n*=4 (2 months), *n*=8 (3 months). Statistical significance was determined using *t*-test comparisons assuming unequal variance. Error bars indicate s.d. (**C-E**) Sections through TEBs in a wild-type gland at 6 weeks of age (C), and through *reeler* (D), and *Dab1* (E) mutant glands at 2 months of age. Cap cells (arrows) are seen at the distal tip of all three TEBs and the transition point from cap cells to myoepithelial cells is marked with arrowheads. WT, wild type.

Table 1. The average ratio of TEBs to total terminal branches

	TEB/branch ratio (*n*)		
Age	Wild type	*Rl*$^{-/-}$	*Dab1*$^{-/-}$
6 weeks	0.337 (7)	0.677 (7)	0.401 (5)
2 months	0.028 (9)	0.289 (7)	0.125 (4)
3 months	0.000 (6)	0.000 (8)	0.200 (8)

To establish an estimate of the stage of maturity of the glands, we determined the average ratio of TEBs to total terminal branches (Table 1). At 6 weeks of age, wild-type glands had an average ratio of 0.337 (*n*=7), decreasing to 0.028 at 2 months and 0.000 at 3 months, reflecting the maturity of the glands. In comparison, *reeler* mutant glands at 6 weeks of age had a ratio of 0.667 (*n*=7), which decreased to 0.289 (*n*=7) at 2 months of age and to 0.000 (*n*=8) at 3 months of age. *Dab1* mutants showed a similar decrease in TEB/branch ratio from 0.401 (*n*=5) at 6 weeks and 0.125 (*n*=4) at 2 months, but four of eight glands still had visible terminal end buds at 3 months of age, producing a TEB/branch ratio of 0.200 (*n*=8). These ratios suggest that *reeler* and *Dab1* mutant glands are still undergoing ductal elongation at 2 months of age. By 3 months of age, TEBs were not present in any *reeler* glands, even in those with rudimentary or immature ductal trees. However, some *Dab1* mutant glands with rudimentary or immature ductal networks still had visible TEBs. These data suggest that gland maturation is complete in *reeler* mutants by 3 months of age, despite the lack of complete ductal trees. However, *Dab1* mutants might retain the capacity for continued development.

We also counted the number of terminal branches, which were defined as distal ductal segments exceeding 100 μm in length, present in each gland. At 6 weeks of age, all branches were counted, whereas at 2 and 3 months of age, only those branches distal to the inguinal lymph node were counted. At all ages, there were on average fewer branches in both *reeler* and *Dab1* mutants compared with controls (Fig. 5B). However, the range of branches was variable in mutant animals, with some animals having near normal numbers of branches, whereas others showed significantly reduced branch numbers. This is evidenced by the large standard deviations seen in the *reeler* and *Dab1* mutant samples.

Alterations in ductal morphogenesis are not due to maternal hormonal status

Reeler and *Dab1* mutant mice display altered nervous system anatomy along with somewhat stunted growth at younger ages. However, despite grossly abnormal morphology, many local and long-distance neural circuits are established correctly (Simmons and Pearlman, 1983; Yip et al., 2003). The brain abnormalities and the reduced body size suggest that hormonal functions governed by the brain might be adversely affected in mutant animals. To test this, we performed mammary gland transplantation to introduce mutant mammary gland tissue into a wild-type environment. We found that in five out of six glands, wild-type transplanted tissue generally formed a robust ductal network. By contrast, in five out of six *Dab1* mutant transplants, transplanted tissue was visible, but mutant tissue either failed to generate a ductal network, or, at best, formed a few rudimentary ducts (Fig. 6). The failure of *Dab1*$^{-/-}$ epithelium to generate a ductal network, either in situ or following transplantation into a wild-type environment, suggests that ductal development is intrinsically impaired in the absence of a functional reelin signaling pathway, and that global changes in hormonal levels are not responsible for the observed phenotypes.

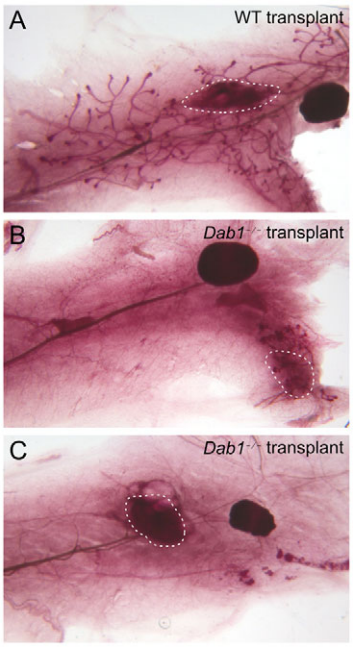

Fig. 6. Mutant tissue transplanted into wild-type hosts fails to elaborate a ductal network. (**A**) Mammary ducts extend from a fragment of a wild-type gland (outlined) in the cleared fat pad of a wild-type host. (**B**,**C**) Transplanted *Dab1* mutant gland fragments (outlined) fail to extend ducts (C) or extend only rudimentary ducts (B).

Loss of reelin signaling alters ductal wall morphology

At 6 weeks of age, wild-type glands had a significant number of ducts visible within the mammary stroma in histological sections (Fig. 7). Ductal profiles were rounded or oval, with even wall thickness and regularly arranged cell bodies in the walls of the ducts (Fig. 7A). By contrast, *reeler* and *Dab1* mutant animals had few visible ducts, and sections through these ducts revealed abnormally thick and disarrayed ductal walls (Fig. 7B). Many ducts also appeared to be occluded (Fig. 7B″), suggesting a delay or defect in cavitation. At 2 months of age, control glands were colonized with regularly spaced ducts that had smooth, even walls (Fig. 7C). Sections through the ducts revealed well-defined lumens, even at their most distal extent. Luminal cell bodies were arranged in a compact single layer with rounded cellular profiles (Fig. 7C″). By contrast, *reeler* and *Dab1* mutant mice had thickened ductal walls and irregular lumens. Luminal cells appeared to be piled on top of each other, creating a luminal wall that was several cell diameters thick (Fig. 7D″). Also, as seen in 6-week-old animals, the distal ends of some ducts did not have discernible lumens. By 3 months of age, control glands had large numbers of ductal profiles. Most ducts had narrow lumens with smooth, even ductal walls and tightly juxtaposed cellular profiles (Fig. 7E,G). By contrast, *reeler* and *Dab1* mutant glands exhibited a variety of abnormal phenotypes. Some glands had very few ducts, with thicker walls and occluded lumens, similar to those seen at 2 months of age, whereas others had a large number of ducts with swollen, severely distended lumens (Fig. 7F). Ducts with swollen lumens had luminal walls that appeared thinner and lacked the compact arrangement of epithelial cells seen in control animals. Instead, luminal cells had elongate nuclei arranged parallel to the lumen (Fig. 7F′). In addition, these ducts appeared to have thinner layers

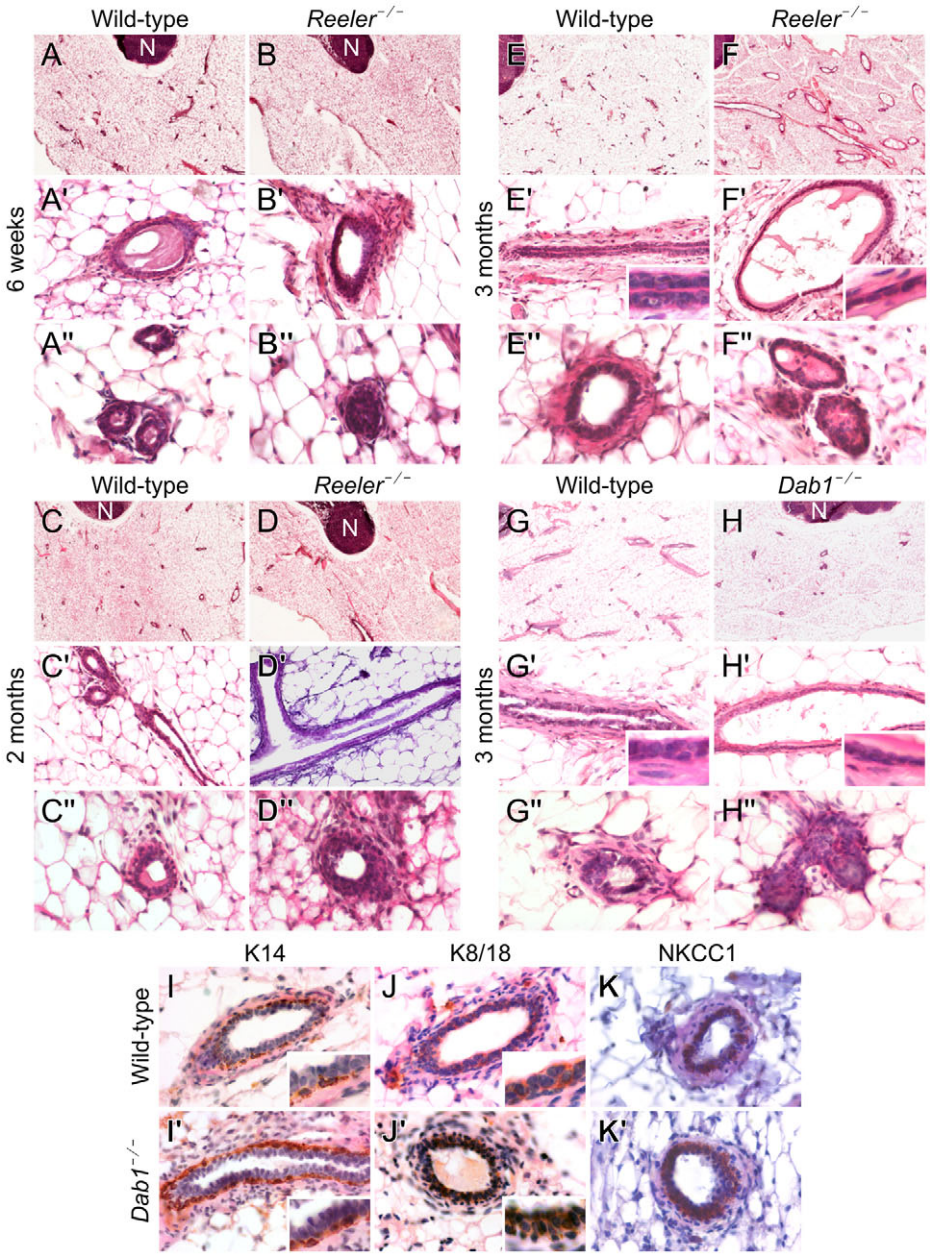

Fig. 7. Mutant mammary ducts have altered morphology. (**A-H**) Low magnification views of hematoxylin and eosin-stained sections taken from inguinal mammary gland #4. (**A′-H′**,**A″-H″**) Higher magnification views of selected ductal profiles from the corresponding section. The inguinal lymph node (N) is included at the top or top left of all low magnification sections for orientation. (**I**,**I′**) K14 expression in wild-type and *Dab1* mutant ducts. (**J**,**J′**) K8/18 expression in wild-type and *Dab1* mutant ducts. (**K**,**K′**) NKCC1 expression in wild-type and *Dab1* mutant ducts. Insets show higher magnification views of the associated panels.

of smooth muscle surrounding the duct. Distal profiles were irregular in shape and many lacked clearly defined lumens (Fig. 7F″,H″).

Ducts from both wild-type and *Dab1* mutant animals at 2 months of age expressed markers for basal cells (K14) and for luminal epithelial cells (K8/18 and NKCC1). K14 labeling was present in the basal cell layer surrounding the luminal epithelial cells in both wild-type and mutant ducts, although labeling appeared somewhat denser in *Dab1* mutant animals, suggesting there may be more basal cells in these mutants (Fig. 7I). K8/18 and NKCC1 were both expressed in luminal epithelial cells (Fig. 7J,K); several layers of cells appeared to express these antigens in mutant animals, whereas a single layer of cells showed expression in wild-type animals. Thus, our results demonstrate that all expected components of the ductal wall are present and identifiable in mutant animals, but that the organization and placement of cells differs in mutants.

Ductal cell proliferation is altered in the absence of reelin signaling

To determine if ductal wall thickening and hypertrophy of the ducts stemmed from changes in the proliferation of ductal cells, we performed Ki67 labeling. As expected, examination of the sectioned profiles in both *reeler* and *Dab1* mutants showed thickened ductal walls and frequent occluded tubules. Ki67-positive cells were prevalent in both thickened tubule walls and in occluded ducts in *Dab1* mutants (Fig. 8F,H), suggesting a relatively high rate of cell proliferation in both of these types of structures. This suggests that the increased thickness of the tubule walls may stem from increased cell proliferation in the mammary epithelium. By contrast, *reeler* mice had few Ki67-positive cells in either type of profile (Fig. 8E,G). In these animals, cell proliferation may have occurred at earlier ages, producing the thickened ductal walls and occluded tubules that are present in these mutants. We then quantified the percentage of Ki67-positive cells in wild-type and

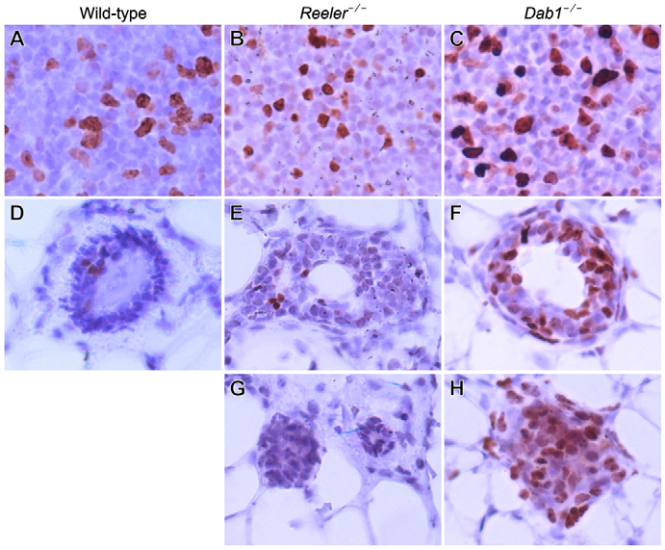

Fig. 8. Ki67 labeling shows altered proliferation in mutant ducts. (**A**,**D**) Wild-type inguinal lymph node (A) and mammary duct (D) labeled for Ki67 expression (brown label). (**B**,**E**,**G**) Ki67 labeling of lymph node (B) and mammary ducts (E,G) in *reeler* mutant. (**C**,**F**,**H**) Ki67 labeling of lymph node (C) and mammary ducts (F,H) in *Dab1* mutant. Occluded ducts were seen in both *reeler* (G) and *Dab1* (H) mutants. All sections are from animals at 3 months of age.

mutant animals (Table 2). As a baseline measure of proliferation, we counted the number of Ki67-positive profiles in sections through the lymph nodes. Baseline proliferation rates appeared somewhat lower in mutant animals than in wild-type animals (Fig. 8), so we determined the ratio of proliferating cells in the mammary ducts vs proliferation in the lymph nodes for further comparisons. In wild-type mammary ducts, an average of 8.75% of the total number of cells was labeled with Ki67, compared with an average of 16.76% of cells in the lymph node, producing a ratio of 0.522. This rate of proliferation probably reflects the normal turnover of cells in the mature mammary epithelium. In *reeler* mutants, only 1.7% of cells in the mammary ducts were labeled with Ki67, compared with 9.7% in the lymph node (ratio=0.175). By contrast, in *Dab1* mutant mice, 14.5% of cells in the mammary ducts were labeled, along with 13.9% of cells in the lymph node (ratio=1.043). These results suggest a very low level of cell proliferation in *reeler* mutants, but an increased rate of proliferation in *Dab1* mutants.

MEC migration is inhibited in the absence of reelin signaling

Because reelin signaling is known to be instrumental in regulating neuronal migration, we wondered whether it might have a similar function in regulating the migration of MECs. Therefore, we isolated wild-type MECs and examined their migration in transwell assays in the presence or absence of soluble reelin. MECs showed significantly reduced migration in the presence of reelin-secreting pCrl cells or pCrl-conditioned media (Fig. 9). We noted a more prominent reduction in MEC migration in the presence of pCrl-conditioned medium (Fig. 9) that may be due to a higher concentration of reelin in conditioned media than in live cell culture.

Table 2. The percentage of Ki67-positive cells in wild-type and mutant mice

	Percentage of Ki67-labeled cells (*n*)		
Genotype	Lymph node	Mammary ducts	Ratio
Wild type	16.76 (8)	8.75 (19)	0.522
Rl$^{-/-}$	9.7 (4)	1.7 (9)	0.175
Dab1$^{-/-}$	13.9 (4)	14.5 (19)	1.043

We performed similar experiments using MECs isolated from *reeler* mutants (Fig. 9). In this experiment, we expected that *reeler* mutant MECs would behave like wild-type cells, as the cellular machinery permitting a response to reelin signaling should be intact in these cells. As shown in Fig. 9, *reeler* mutant MECs behaved similarly to wild-type MECs, with reduced migration in the presence of pCrl cells or conditioned medium. Again, a greater reduction in migration was observed with conditioned medium than with live cell cultures.

We also performed the same experiment using MECs isolated from *Dab1* mutants. We expected that *Dab1* mutant cells would not respond to the presence of reelin in the transwells, as disruption of the *Dab1* gene ablates the canonical reelin signaling pathway cell autonomously. *Dab1* mutant MEC migration was not impeded either by the presence of pCrl cells or by pCrl-conditioned media. The migration rate of *Dab1* mutant cells even appeared to increase slightly in the presence of pCrl cells or conditioned media, although these increases were not statistically significant. These observations support the hypothesis that reelin may act directly on MECs to limit their migration, and that disrupting the reelin signaling pathway abrogates the effect of reelin on MEC migration.

DISCUSSION

Several lines of evidence support a role for reelin signaling in mammary gland morphogenesis. First, disruption of the reelin signaling pathway in both *reeler* and *Dab1* mutants alters ductal development and arborization. Second, transplantation studies demonstrate a requirement for intact reelin signaling in promoting ductal outgrowth. Third, reelin has direct and demonstrable effects on the migration of mammary epithelial cells. Taken together, these observations suggest a pivotal role for reelin signaling in regulating mammary ductal development.

The molecular mechanisms of reelin signaling have been widely studied in the central nervous system. Extracellular reelin binds to ApoER2 and VLDLR receptors, triggering the phosphorylation of Dab1 and initiating a cascade of events leading to microtubule stabilization (reviewed by Herz and Chen, 2006). The expression of reelin, ApoER2, VLDLR and Dab1 in and around the mammary bud and in the luminal epithelial and periductal stroma of the mature gland suggests that an identical chain of events is utilized in the mammary gland. The early distribution of Dab1 and reelin suggests that reelin expressed in the epithelium may regulate the migration or positioning of Dab1-expressing cells in the invaginating mammary bud; however, loss of *reelin* or *Dab1* does not disrupt early mammary bud development.

In the maturing gland, reelin was expressed in the periductal stroma and myoepithelial layers surrounding the luminal epithelium, whereas Dab1 was expressed in a complementary pattern in the luminal epithelium. This arrangement suggests that reelin from the stromal and myoepithelial layers might provide a signal to the Dab1-expressing cells in the luminal epithelium. Reelin is a large extracellular matrix glycoprotein (D'Arcangelo et al., 1995); therefore, one possibility is that reelin is a component of the

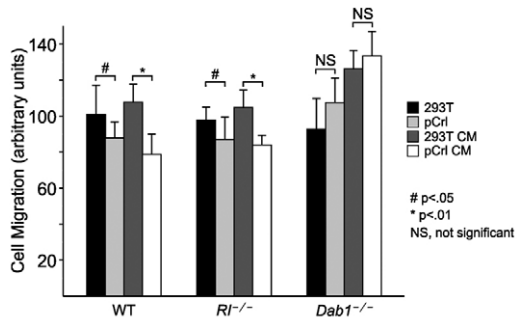

Fig. 9. Exogenous reelin inhibits MEC migration. Migration of primary MECs in transwell assays. Wild-type, *Rl*$^{-/-}$ or *Dab1*$^{-/-}$ MECs were introduced into transwells in the presence of control cells, control conditioned medium, reelin-secreting cells or reelin-secreting cell conditioned medium. Mean cell migration rate was calculated as a percentage of the migration rate observed in the presence of DMEM+FBS alone; error bars indicate s.d. Statistical significance was determined using two-sample *t* test comparisons assuming equal variance. 293T, control cells; 293T CM, control conditioned medium; pCrl, reelin-secreting cells; pCrl CM, reelin-secreting cell conditioned medium.

mammary gland extracellular matrix (ECM). Interactions between luminal epithelial cells and the surrounding ECM are crucial for directing epithelial organization and cavitation, as well as for establishing the position of ductal branch points (reviewed by Gjorevski and Nelson, 2009). During cavitation, luminal cells that maintained contact with the basal lamina persisted, whereas detachment from the basal lamina led to apoptosis, leaving an organized epithelium surrounding a hollow central lumen. In the absence of reelin signaling, mammary ducts developed thick, multilayered walls and often remained occluded. These phenotypes suggest disruption of interactions between the luminal epithelial cells and the ECM, such that the signals necessary to induce apoptosis are not properly transmitted, leading to the presence of occluded ducts. In contrast to the thickened walls and lack of cavitation, some ducts appeared distended, with thin epithelial walls. Bloating of these ducts may be caused by a lack of structural integrity in the epithelial walls also as a result of disrupted matrix interactions; the epithelial walls then become distended due to pressure from the lumen.

Thickened ductal walls and occluded tubules suggest that additional cells are present in the mutant ducts. The additional cells could reflect a failure in cell death, as might be produced by disruptions in the interactions with the ECM, or might reflect increased cell proliferation. Ki67 labeling suggests an increased rate of cell proliferation in *Dab1* mutant glands, lending some credence to the second hypothesis. However, this increased cell proliferation might also indicate an earlier phase of ductal development, suggesting that *Dab1* mutant ducts are less mature than comparably aged *reeler* or wild-type ducts. If this is the case, then one might expect that rates of cell proliferation would decrease in older glands, and this remains to be tested. Alternatively, if high rates of cell proliferation are retained at later ages, then these cells might represent carcinoma in situ. Loss of reelin signaling has been linked to increased motility and invasiveness in pancreatic cancer (Sato et al., 2006); similar activities might occur in the mammary gland. Owing to the limited survival of older mutant animals, it remains to be seen if mammary tumors develop at a higher rate in *reeler* or *Dab1* mutants.

One possible explanation for the observed mammary gland phenotypes might be a global delay in development. *Reeler* and *Dab1* mutant mice are generally smaller than wild-type mice and have abnormal brain structures that could result in disruptions in hormone production and/or secretion, altering mammary gland development (Hennighausen and Robinson, 2005). Whereas these processes could be contributing factors, particularly to the early delays in ductal morphogenesis observed in virtually all mutant mice, our transplantation studies suggested that the probable cause of later phenotypes, including decreased branching and ductal wall abnormalities, is the intrinsic disruption of reelin signaling. The retraction of TEBs in mutants, even in the absence of complete ductal elongation, suggested that maturation of the gland had occurred and that limited ductal arborization was a persistent and permanent phenotype. TEBs depend on signals from a variety of growth factors, including IGF-1, growth hormone and sex steroids (Kleinberg and Ruan, 2008), and these signals may also be disrupted in *reeler* and *Dab1* mutants.

The isolation of mammary stem cells (MaSCs) (Shackleton et al., 2006) illustrates a key player in the expansion of the ductal network during puberty and pregnancy. MaSC expansion is normally restricted by Notch signaling (Bouras et al., 2008). Recent findings in the CNS suggest that Notch is a downstream mediator of reelin signaling (Hashimoto-Torii et al., 2008). In the mammary gland, loss of reelin signaling and a concomitant decrease in Notch expression might lead to the expansion of the MaSC population; this might be reflected in the increased K14 expression evident in *reeler* and *Dab1* mutants. However, this might also predict an increase in ductal growth and expansion, which is clearly not seen in these mutants, suggesting that additional signals might be required to stimulate stem cell proliferation and contribution to ductal growth. However, an expanded stem cell population might also predispose mutant ducts to increased tumorigenesis, which remains to be seen.

Our finding that MEC migration was slowed in the presence of reelin suggests a direct effect of reelin signaling on the cellular machinery of MECs. In neurons, reelin signaling initiates a cascade of events, ultimately inhibiting the phosphorylation of tau protein and stabilizing the cytoskeleton (reviewed by Herz and Chen, 2006). Knocking down expression of reelin pathway components increases the migration of pancreatic cancer cells (Sato et al., 2006), and our results showed similar effects on the migration of mammary epithelial cells. Thus, reelin in the extracellular matrix surrounding the developing ducts might serve to inhibit the migration of mammary epithelial cells, constraining these cells to remain within the luminal epithelium. In the absence of reelin signaling, enhanced cell migration could contribute to the abnormal ductal morphology, particularly to the increased thickness of the ductal walls. This phenotype may reflect an effort by mammary epithelial cells to continue migrating, even in the presence of a stabilizing extracellular matrix. This might lead to changes in cell layering, similar to changes seen in the developing brain and evidenced as thickened ductal walls or possibly at later stages to carcinoma in situ.

In summary, we have found a novel, independent role for reelin signaling in mammary gland morphogenesis. Reelin signaling is required for the extension and elaboration of the mammary ductal network, as well as for the organization of the luminal epithelial wall. Loss of reelin signaling results in increased proliferation and migration of luminal mammary epithelial cells; these changes may stem from disrupted interactions with the extracellular matrix. These studies demonstrate an important role for reelin signaling in

shaping the mammary gland and provide the first evidence that reelin signaling may be crucial for regulating the migration and organization of non-neural tissues.

Acknowledgements
We thank J. Colicelli and P. Phelps for helpful discussions and critical reading of the manuscript; D. Anthony, J. Phillips and K. Bui for assistance with cell counting; E. Kirkbride for assistance with RT-PCR; J. Han, J. Stevens and J. Huang for assistance with immunohistochemistry; and D. Crandall for assistance with figure preparation. This research was supported by the UCLA Stein/Oppenheimer Endowment and by grants from the NIH (HD061815) and the California Breast Cancer Research Program (161B-0110) to E.M.C. Deposited in PMC for release after 12 months.

Competing interests statement
The authors declare no competing financial interests.

References
Anderson, T. R., Hedlund, E. and Carpenter, E. M. (2002). Differential *Pax6* promoter activity and transcript expression during forebrain development. *Mech. Dev.* **114**, 171-175.
Ball, S. (1998). The development of the terminal end bud in the prepubertal-pubertal mouse mammary gland. *Anat. Rec.* **250**, 459-464.
Bouras, R., Pal, B., Vaillani, F., Harburg, G., Asselin-Labat, M.-L., Oakes, S. R., Lindeman, G. J. and Visvader, J. E. (2008). Notch signaling regulates mammary stem cell function and luminal cell-fate commitment. *Cell Stem Cell* **3**, 429-441.
Caviness, V. S. (1976). Patterns of cell and fiber distribution in the neocortex of the reeler mutant mouse. *J. Comp. Neurol.* **170**, 435-447.
Caviness, V. S. and Sidman, R. L. (1973). Retrohippocampal, hippocampal and related structures of the forebrain in the reeler mutant mouse. *J. Comp. Neurol.* **147**, 235-254.
Costagli, A., Felice, B., Guffanti, A., Wilson, S. W. and Mione, M. (2006). Identification of alternatively spliced dab1 isoforms in zebrafish. *Dev. Genes Evol.* **216**, 291-299.
Cunha, G. R. (1994). Role of mesenchymal-epithelial interactions in normal and abnormal development of the mammary gland and prostate. *Cancer* **74**, 1030-1044.
D'Arcangelo, G. and Curran, T. (1998). Reeler: new tales on an old mouse mutant. *BioEssays* **20**, 235-244.
D'Arcangelo, G., Miao, G. G., Chen, S. C., Soares, H. D., Morgan, J. I. and Curran, T. (1995). A protein related to extracellular matrix proteins deleted in the mouse mutant reeler. *Nature* **374**, 719-723.
D'Arcangelo, G., Homayouni, R., Keshvara, L., Rice, D. S., Sheldon, M. and Curran, T. (1999). Reelin is a ligand for lipoprotein receptors. *Neuron* **24**, 471-479.
DeOme, K. B., Faulkin, L. J., Jr, Bern, H. A. and Blair, P. B. (1959). Development of mammary tumors from hyperplastic alveolar nodules transplanted into gland-free mammary fat pads of female C3H mice. *Cancer Res.* **19**, 515-520.
Förster, E., Jossin, Y., Zhao, S., Chai, X., Frotscher, M. and Goffinet, A. M. (2006). Recent progress in understanding the role of Reelin in radial neuronal migration, with specific emphasis on the dentate gyrus. *Eur. J. Neurosci.* **23**, 901-909.
Gjorevski, N. and Nelson, C. M. (2009). Bidirectional extracellular matrix signaling during tissue morphogenesis. *Cytokine Growth Factor Rev*. **20**, 459-465.
Goffinet, A. M. (1984). Events governing organization of postmigratory neurons: studies on brain development in normal and reeler mice. *Brain Res.* **319**, 261-296.
Goffinet, A. M., So, K. F., Yamamoto, M., Edwards, M. and Caviness, V. S. (1984). Architectonic and hodological organization of the cerebellum in reeler mutant mice. *Brain Res.* **318**, 263-276.
Hashimoto-Torii, K., Torii, M., Sarkisian, M. R., Bartley, C. M., Shen, J., Radtke, F., Gridley, T., Sestan, N. and Rakic, P. (2008). Interaction between reelin and notch signaling regulates neuronal migration in the cerebral cortex. *Neuron* **60**, 273-284.
Hennighausen, L. and Robinson, G. W. (2005). Information networks in the mammary gland. *Nat. Rev. Mol. Cell. Biol.* **6**, 715-725.
Herz, J. and Chen, Y. (2006). Reelin, lipoprotein receptors and synaptic plasticity. *Nat. Rev. Neurosci.* **7**, 850-859.
Howell, B. W., Gertler, F. B. and Cooper, J. A. (1997a). Mouse disabled (mDab1): a Src binding protein implicated in neuronal development. *EMBO J.* **16**, 121-132.
Howell, B. W., Hawkes, R., Soriano, P. and Cooper, J. A. (1997b). Neuronal position in the developing brain is regulated by mouse disabled-1. *Nature* **389**, 733-737.
Howell, B. W., Herrick, T. M. and Cooper, J. A. (1999). Reelin-induced tyrosine phosphorylation of Disabled 1 during neuronal positioning. *Genes Dev.* **13**, 643-648.
Hu, H., Bliss, J. M., Wang, Y. and Colicelli, J. (2005). RIN1 is an ABL tyrosine kinase activator and a regulator of epithelial-cell adhesion and migration. *Curr. Biol.* **15**, 815-823.
Kleinberg, D. L. and Ruan, W. (2008). IGF-1, GH, and sex steroid effects in normal mammary gland development. *J. Mammary Gland Biol. Neoplasia* **13**, 353-360.
Kuo, G., Arnaud, L., Kronstad-O'Brien, P. and Cooper, J. A. (2005). Absence of Fyn and Src causes a reeler-like phenotype. *J. Neurosci.* **25**, 8578-8586.
Li, G., Robinson, G. W., Lesche, R., Martinez-Diaz, H., Jiang, Z., Rozengurt, N., Wagner, K.-U., Wu, D.-C., Lane, T. F., Liu, X. et al. (2002). Conditional loss of PTEN leads to precocious development and neoplasia in the mammary gland. *Development* **129**, 4159-4170.
Maurin, J. C., Couble, M. L., Didier-Bazes, M., Brisson, C., Magloire, H. and Bleicher, F. (2004). Expression and localization of reelin in human odontoblasts. *Matrix Biol.* **23**, 277-285.
Mikkola, M. L. and Millar, S. E. (2006). The mammary bud as a skin appendage: unique and shared aspects of development. *J. Mammary Gland Biol. Neoplasia* **11**, 187-203.
Naylor, M. J. and Ormandy, C. J. (2002). Mouse strain-specific patterns of mammary epithelial ductal side branching are elicited by stromal factors. *Dev. Dyn.* **225**, 100-105.
Phelps, P. E., Rich, R., Dupuy-Davis, S., Rios, Y. and Wong, T. (2002). Evidence for a cell-specific action of Reelin in the spinal cord. *Dev. Biol.* **244**, 180-198.
Pramatarova, A., Chen, K. and Howell, B. W. (2008). A genetic interaction between the APP and Dab1 genes influences brain development. *Mol. Cell. Neurosci.* **37**, 178-186.
Rice, D. S. and Curran, T. (2001). Role of the Reelin signaling pathway in central nervous system development. *Annu. Rev. Neurosci.* **24**, 1005-1039.
Robinson, G. W. (2007). Cooperation of signaling pathways in embryonic mammary gland development. *Nat. Rev. Genet.* **8**, 963-972.
Sato, N., Fukushima, N., Chang, R., Matsubayashi, H. and Goggins, M. (2006). Differential and epigenetic gene expression profiling identifies frequent disruption of the RELN pathway in pancreatic cancers. *Gastroenterology* **130**, 548-565.
Shackleton, M., Vaillant, F., Simpson, K. J., Stingl, J., Smyth, G. K., Asselin-Labal, M.-L., Lindeman, G. J. and Visvader, J. E. (2006). Generation of a functional mammary gland from a single stem cell. *Nature* **439**, 84-88.
Simmons, P. A. and Pearlman, A. L. (1983). Receptive-field properties of transcallosal visual cortical neurons in the normal and reeler mouse. *J. Neurophysiol.* **50**, 838-848.
Sternlicht, M. D., Kouros-Mehr, H., Lu, P. and Werb, Z. (2006). Hormonal and local control of mammary branching morphogenesis. *Differentiation* **74**, 365-381.
Streuli, C. H., Schmidhauser, C., Bailey, N., Yurchenco, P., Skubitz, A. P., Roskelley, C. and Bissell, M. J. (1995). Laminin mediates tissue-specific gene expression in mammary epithelia. *J. Cell Biol.* **129**, 591-603.
Yip, J. W., Yip, Y. P., Nakajima, K. and Capriotti, C. (2000). Reelin controls position of autonomic neurons in the spinal cord. *Proc. Natl. Acad. Sci. USA* **97**, 8612-8616.
Yip, Y. P., Rinaman, L., Capriotti, C. and Yip, J. W. (2003). Ectopic sympathetic preganglionic neurons maintain proper connectivity in the reeler mutant mouse. *Neuroscience* **118**, 439-450.